An Integrated Topology of Hybrid Marine Farm & Wind Farm

Mohammad Hasanuzzaman Shawon*‡, Subarto Kumar Ghosh*, Md. Ashifur Rahman*

*Department of E.E.E, Daffodil International University

shawon@daffodilvarsity.edu.bd, subarto@daffodilvarsity.edu.bd, arahman@daffodilvarsity.edu.bd

‡ Corresponding Author; Mohammad Hasanuzzaman Shawon, Department of E.E.E, Senior Lecturer, Daffodil International University, Dhaka, Bangladesh, shawon@daffodilvarsity.edu.bd

Received: 04.01.2013 Accepted: 26.04.2013

Abstract- Renewable energy has been playing an important role to meet power demand and 'Green Energy' market is getting bigger platform all over the world in the last few years. In order to meet the increasing demand of electricity and power, integration of renewable energy is getting highest priorities around the world. Wind is one of the most top growing renewable energy resources and it is the most environmental friendly, cost effective and safe among all renewable energy resources available. Another promising form of renewable energy is ocean energy which covers 70 % of the earth. Offshore Wind farm` (OWF) has already become very popular for large scale wind power integration with the onshore grid. Recently, marine current farm (MCF) is also showing good potential to become mainstream energy sources and already successfully commissioned in United Kingdom. An integration of wind and tidal energy represents a new-trend for large electric energy production using offshore wind generators and marine current generators, respectively. This work first focuses on the modeling of fixed speed IG based marine current farm and variable speed DFIG based wind farm. Detailed modeling and control scheme for the proposed system are demonstrated considering some realistic scenarios. The power system small signal stability analysis is also carried out by eigenvalue analysis for marine current generator topology, wind turbine generator topology and integrated topology. The relation between the modes and state variables are discussed in light of modal and sensitivity analyses. The results of theoretical analyses are verified by MATLAB/SIMULINK.

Keywords- Marine Energy; Wind Energy; Induction Machine; Stability; Eigen Value.

1. Introduction

In order to conserve the non-renewable energy resources as well as to reduce Carbon footprint all over the world, science and technology have led us to explore the new resources for electricity generation which is clean, safe and capable of serving the society for a long period. A wind energy system is the most environmental friendly, cost effective and safest among all renewable energy resources available [1]. It has been forecasted that the increase in electricity generation from renewable sources between 2008 and 2035 will be primarily derived from wind and hydro power, which will contribute 36% and 31% of the additional demand respectively [2]. Wind power is projected to supply 8% of global electricity in 2035 up from just 1% in 2008. In the year 2010, the wind capacity has reached 196.630GW worldwide and it will reach 240GW by the end of 2012 [3]. Ocean energy is also considered as an abundant and non-pollution energy resource [4]. Various wave and tidal projects have been established all over the world to harness the energy from the sea. In 2007, the first commercial tidal steam converter, the "SeaGen", started operation in Northern Ireland [5]. Along with the development of researches on wind power technology, the small signal stability of wind power generation is getting remarkable importance, in the recent years. Small signal stability analysis of the power system including the widely used synchronous machine is a well-developed field of study [6-8]. Effect of wind energy conversion system on small signal stability model along with conventional power system equipped with synchronous generator and power system stabilizer (PSS) is presented in [9]. The small signal dynamic models for both fixed and variable speed wind turbine generator systems are available in power system literatures [10-12]. The dynamic and transient behavior of fixed and variable speed generator is presented in [13]. In [14], oscillatory stability and eigenvalue sensitivity of doubly fed induction generator (DFIG) based wind power generation system is presented. Dynamic behavior analysis and influence of reactive power and speed controller parameters of DFIG is discussed in [15]. Effects of damping controller on the different modes as well as super/sub synchronous modes of operation of DFIG have been investigated in [16]. However, analysis of integrated topology of wind energy generation and marine energy generation and interaction of different dynamic modes based on modal and frequency domain analyses have not been reported much. This work is intended to present a comprehensive study of small signal stability of the IG based fixed speed marine current generator as well as DFIG based variable speed wind turbine generator connected to a power grid.

2. Generator Marine Current System

2.1. System Overview

The fixed speed marine current farm comprises a squirrel cage induction generator where the stator winding of IG is directly connected to the power grid through capacitor bank and double-circuit transmission line.

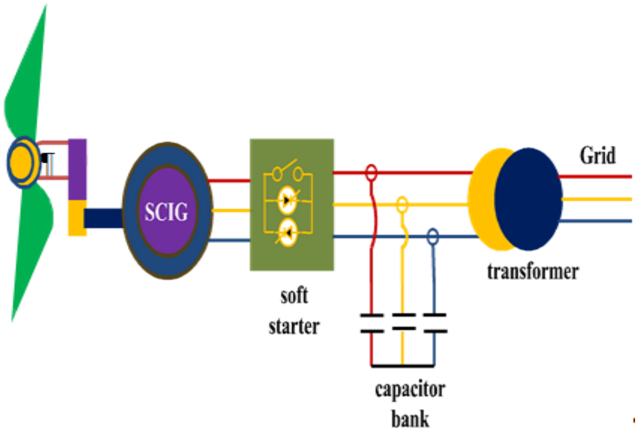

Fig. 1. Schematic diagram of marine energy system

2.2. Marine Turbine

The amount of mechanical power Pm captured from ocean can be expressed by the following equation [18].

$$P_m = \frac{1}{2}.\rho_m.A_m.V_m^3.C_{pm}(\lambda_m, \beta_m) \quad (1)$$

Where ρ_m is the ocean current density [kg/m^3], A_m is the area of turbine blade [m^2], V_m is marine current speed [m/s], C_{pm} is the power coefficient, λ_m is tip speed ratio and β is pitch angle [degree]. Equation for C_{pm} is described as below:

$$C_{pm}(\psi_m, \beta_m) = \left[d_1 (\frac{d_2}{\psi_m} - d_3\beta_m - d_4\beta_m^{d^5} - d_6) \right] . \exp\left[-\frac{d_7}{\psi_m} \right] \quad (2)$$

The relationship between λ , β and Ψm are

$$\lambda_m = \frac{R_{bm}.\omega_m}{V_m} \quad (3)$$

$$\frac{1}{\psi_m} = \frac{1}{\lambda_m + d_8\beta_m} - \frac{d_9}{\beta_m^3 + 1} \quad (4)$$

where ω_{bm} is the blade angular velocity [rad/s], R_{bm} is the blade radius [m] and d_1-d_9 are the constant coefficient of C_{pm}. Rated speed of marine turbine is considered as 2.72 m/s.

2.3. Drive Train

The Drive train modeling has been accomplished considering the inertia of generator and turbine while connecting shaft is modeled as a damper and a spring. Figure 2 shows detailed and simplified two-mass drive train models of marine turbine generator system. This study considers the simplified two-mass model which is sufficient for dynamic and transient analyses [19-20].The two mass model can be expressed by:

$$(2H_{tm})\frac{d\omega_{tm}}{dt} = T_m - K_{sm}\theta_m - D_m(\omega_{tm} - \omega_{rm}) \quad (5)$$

$$(2H_{rm})\frac{d\omega_{rm}}{dt} = T_e + K_{sm}\theta_m + D(\omega_{tm} - \omega_{rm}) \quad (6)$$

$$\frac{d\theta_m}{dt} = \omega_{bm}(\omega_{tm} - \omega_{rm}) \quad (7)$$

where ω_{tm} and ω_{rm} is the pu angular speed of the turbine and IG, respectively, D_m, $K_{sm,}$ and θ_m are the mechanical damping coefficient [pu], spring constant [pu], and rotor angle [pu] difference between marine turbine and the IG [pu], respectively. H_{tm} and H_{rm} are the inertia constants (in seconds) of marine turbine and the IG, respectively. T_e and T_m are the electromagnetic and mechanical torques, respectivel.

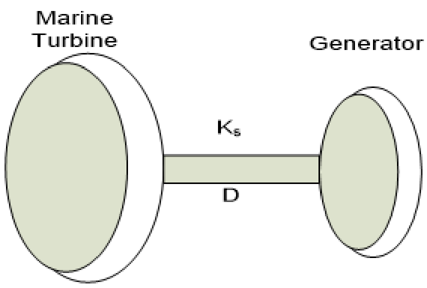

Fig. 2. Drive train models for marine turbine:simplified two-mass model

2.4. Drive Train

Figure 3 shows equivalent circuit of squirrel cage induction generator based on synchronously rotating reference frame. The d and q axis stator fluxes and rotor currents are chosen as state variables.

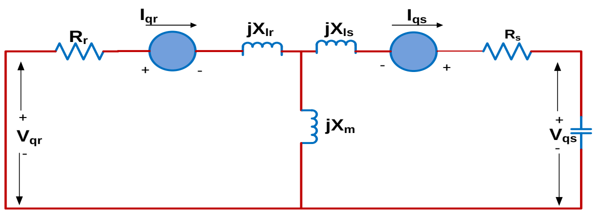

(a)

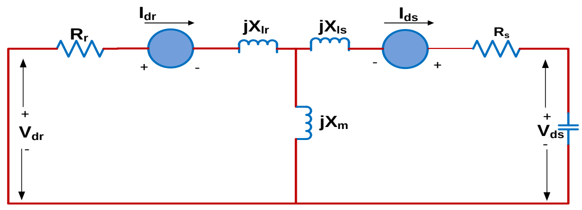

(b)

Fig. 3. Equivalent model of the induction generator: (a) q-axis and (b) d-axis representation.

The electrical quantities of induction machine can be expressed by the following equations: [21,22]:

$$V_{sd} = R_s I_{sd} - \omega_s \psi_{sq} + \frac{1}{\omega_b}\frac{d\psi_{sd}}{dt} \quad (8)$$

$$V_{sq} = R_s I_{sq} + \omega_s \psi_{sd} + \frac{1}{\omega_b}\frac{d\psi_{sq}}{dt} \quad (9)$$

$$V_{rd} = R_r I_{rd} - \omega_2 \psi_{rd} + \frac{1}{\omega_b}\frac{d\psi_{rd}}{dt} \quad (10)$$

$$V_{rq} = R_r I_{rq} + \omega_2 \psi_{rd} + \frac{1}{\omega_b}\frac{d\psi_{rq}}{dt} \quad (11)$$

$$\psi_s = L_s I_s + L_m I_r \quad (12)$$

$$\psi_r = L_m I_s + L_r I_r \quad (13)$$

$$T_e = \frac{L_m}{L_s}(\psi_{sq} I_{rd} - \psi_{sd} I_{rq}) \quad (14)$$

Now, from equation (8-14), state space representation of IG can be written as a function of state variables:

$$\frac{1}{\omega_b}\frac{d\psi_{sd}}{dt} = -\frac{R_s}{L_s}\psi_{sd} + \frac{R_s L_m}{L_m} I_{rd} + \omega_s \psi_{sq} + V_{sd} \quad (15)$$

$$\frac{1}{\omega_b}\frac{d\psi_{sq}}{dt} = -\frac{R_s}{L_s}\psi_{sq} + \frac{R_s L_m}{L_m} I_{rq} - \omega_s \psi_{sd} + V_{sq} \quad (16)$$

$$\frac{L_r'}{\omega_b}\frac{dI_{rd}}{dt} = -R_r' I_{rd} + \frac{R_s L_m}{L_s^2}\psi_{sd} - \frac{L_m}{L_s}\omega_r \psi_{sq} + L_r' \omega_2 I_{rq} - \frac{L_m}{L_s} V_{sd} \quad (17)$$

$$\frac{L_r'}{\omega_b}\frac{dI_{rq}}{dt} = -R_r' I_{rq} + \frac{R_s L_m}{L_s^2}\psi_{sq} + \frac{L_m}{L_s}\omega_r \psi_{sd} - L_r' \omega_2 I_{rd} - \frac{L_m}{L_s} V_{sq} \quad (18)$$

where V_s and V_r are stator and rotor pu voltage, L_m is the pu mutual inductance, L_s and L_r are stator and rotor pu self inductance, R_s and R_r are stator and rotor pu resistance, $\Psi_s$and $\Psi_r$are stator and rotor pu flux, ω_s, ω_r, ω_2 are synchronous angular frequency, rotor angular frequency, and rotor slip frequency (all in pu), ω_b is the base angular frequency [377 rad/sec] and T_e is pu electromagnetic torque.

2.5. Transmission Line and Capacitor Bank

A capacitor bank is connected at terminal of induction generator at rated condition which can be expressed by the following state equation in terms of capacitor voltage.

$$C\frac{dV_{sd}}{dt} = (-\frac{1}{L_s}\psi_{sd} + \frac{L_m}{L_s} I_{rd} + I_{dt} + C\omega_s V_{sq})\omega_b \quad (19)$$

$$C\frac{dV_{sq}}{dt} = (-\frac{1}{L_s}\psi_{sq} + \frac{L_m}{L_s} I_{rq} + I_{qt} - C\omega_s V_{sd})\omega_b \quad (20)$$

where C is the capacitance bank value, I_{dt} and I_{qt} are the pu d-axis and q-axis transmission line current, respectively. The d-q axis current equations for the equivalent transmission line can be expressed by the following state equation:

$$L_t\frac{dI_{dt}}{dt} = (-V_{sd} - R_t I_{dt} + L_t \omega_s I_{qt} + V_{gd})\omega_b \quad (21)$$

$$L_t\frac{dI_{qt}}{dt} = (-V_{sq} - R_t I_{qt} - L_t \omega_s I_{dt} + V_{gq})\omega_b \quad (22)$$

where R_t and L_t are equivalent resistance and inductance of the transmission line, respectively and V_{gd} and V_{qd} are the d-axis and q-axis pu grid voltages, respectively, all in pu.

3. Generator Marine Current System

3.1. System Overview

The wind turbine generator system comprises a doubly fed induction generator which connected to power grid through the transmission line which may include the impedance of transformer and connection cable. The schematic diagram of DFIG connected with power grid is present in Fig. 4. The DFIG based wind power system is modeled using 5th order machine model in which stator and rotor dynamics are considered.

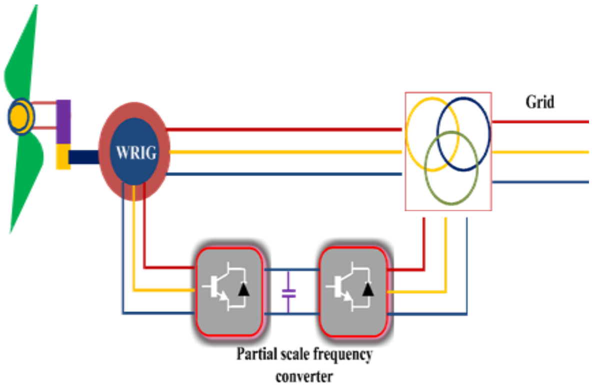

Fig. 4. Schematic diagram of the variable speed wind turbine generator system

3.2. Wind Turbine, Drive Train and MPPT

The electrical The wind turbine system comprises a prime mover, a shaft and a gearbox unit. The dynamic interaction involving forces from the wind and the responses of wind turbine determines the amount of kinetic energy that can be extracted. The amount of mechanical power P_w extracted from wind can be expressed by the following equation [23].

$$P_w = \frac{1}{2}.\rho_w.A_w.V_w^3.C_{pw}(\lambda_w,\beta_w) \quad (23)$$

where ρ_w is the air density [kg/m^3], A_w is the area of turbine blade [m^2], V_w is the wind velocity [m/s], C_{pw} is the power coefficient, λ_w is the tip speed ratio and β_w is the pitch angle [degree]. The power coefficient C_{pw} is given by [24]

$$C_{pw}(\lambda_w,\beta_w) = 0.5(\Gamma - 0.02\beta^2 - 5.6)\exp[-0.17\Gamma] \quad (24)$$

The tip speed ratio, is defined as

$$\lambda_m = \frac{R_{bw}.\omega_w}{V_w} \quad (25)$$

$$\Gamma = \frac{R.(3600)}{\lambda_w} \quad (26)$$

The turbine torque coefficient C_{tw} is related with turbine power coefficient C_{pw} by the equation:

$$C_{tw}(\lambda) = \frac{C_{pw}}{\lambda} \quad (27)$$

$$T_{mw} = \frac{1}{2}.\rho_w.A_w.R_{bw}^3 V_w^2.C_{tw}(\lambda) \quad (28)$$

where R_{bw} is the blade radius [m], ω_w is the rotational speed [rad/s] and T_{mw} is the wind turbine output torque [Nm].)

Equation 29 and 31 are used to calculate the reference of the active power output and the optimum rotor speed are given in equation 29 and MPPT control block is showed in Figure 6.

$$P_{ref1} = 0.1571V_w - 1.035[\text{pu}] \quad (29)$$

$$P_{ref2} = 0.214771V_w - 1.668[\text{pu}] \quad (30)$$

$$\omega_{opt} = 0.0775[\text{pu}] \quad (31)$$

The two mass model can be expressed by:

$$(2H_{tw})\frac{d\omega_{tw}}{dt} = T_m - K_{sw}\theta_w - D_w(\omega_{tw} - \omega_{rw}) \quad (32)$$

$$(2H_{rw})\frac{d\omega_{rw}}{dt} = T_e + K_{sw}\theta_w + D_w(\omega_{tw} - \omega_{rw}) \quad (33)$$

$$\frac{d\theta_w}{dt} = \omega_{bw}(\omega_{tw} - \omega_{rw}) \quad (34)$$

where ω_{tw} and ω_{rw} is the pu angular speed of the turbine and IG, respectively, D_w, $K_{sw,}$ and θ_w are the mechanical damping coefficient [pu], spring constant [pu], and rotor angle [pu]difference between marine turbine and the IG [pu], respectively. H_{tw} and H_{rw} are the inertia constants (in seconds) of marine turbine and the IG, respectively. T_e and T_m are the electromagnetic and mechanical torques, respectively.

3.3. Doubly Fed Induction Generator

According to stator flux orientation$\Psi_s = \Psi_{sd}$ and $\Psi_{sq} = 0$ [31]. Stator side of DFIG is presented with the help of rotor current, stator flux and stator voltage. Rotor current and stator flux variables can be used to build the state equations of stator model.

$$\frac{1}{\omega_b}\frac{d\psi_{sd}}{dt} = -\frac{R_s}{L_s}\psi_{sd} + \frac{R_s L_m}{L_s}I_{rd} + V_s\cos\gamma \quad (43)$$

$$\frac{d\gamma}{dt} = \omega_b(\omega_s - \omega) \quad (44)$$

where ω_s is synchronous frequency and ω is speed of the dq reference frame, all in pu. γ is denoted as the angle difference between the stator side voltage angle and stator flux angle with respect to stationary reference frame and V_s is the stator voltage [pu].stator and rotor voltages are depicted in terms of same reference frame.

$$V_r = R_r I_r + \frac{1}{\omega_b}\frac{d\psi_r}{dt} + j(\omega_s - \omega_r)\psi_r \quad (45)$$

$$V_s = R_s I_s + \frac{1}{\omega_b}\frac{d\psi_{sd}}{dt} + j\omega_s\psi_s \quad (46)$$

Substituting equation (45) into (46) and including the transient terms of stator flux, the following equation can be obtained

$$\frac{1}{\omega_b}\frac{d\psi_s}{dt} = V_s - \frac{R_s}{L_s}\psi_s + \frac{R_s L_m}{L_s}.I_r - j\omega_s\psi_s \quad (47)$$

$$V_r = R_r I_r + \frac{L_r}{\omega_b}\sigma_r\frac{dI_r}{dt} + \frac{L_m}{L_s}\frac{d\psi_s}{dt} + j\omega_2\sigma L_r I_r + j\omega_2\frac{L_m}{L_s}\psi_s \quad (48)$$

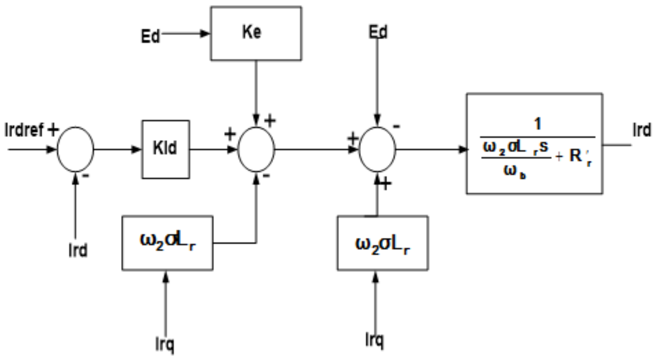

Fig. 5. d-axis rotor current controller

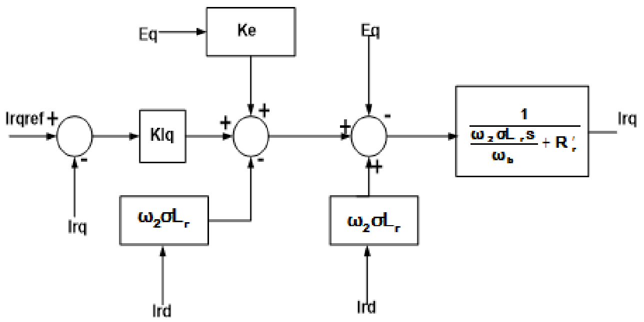

Fig. 6. q-axis rotor current controller

Substituting equation (47) into equation (48),

$$V_r = R'_r I_r + \frac{L_r}{\omega_b}\sigma_r \frac{dI_r}{dt} + + j\omega_2\sigma L_r I_r + \frac{L_m}{L_s}\left(V_s - \frac{R_s}{L_s}\psi_s + j\omega_r\psi_s\right) \quad (49)$$

Rotor voltage equations are rewritten in terms of d-q reference frame in the following equations

$$V_{rd} = R'_r I_{rd} + \frac{L_r}{\omega_b}\sigma_r \frac{dI_{rd}}{dt} + + j\omega_2\sigma L_r I_{rd} + E_d \quad (50)$$

$$V_{rq} = R'_r I_{rq} + \frac{L_r}{\omega_b}\sigma_r \frac{dI_{rq}}{dt} + + j\omega_2\sigma L_r I_{rq} + E_q \quad (51)$$

where E_d and E_q are called rotor back EMF

$$E_d = \frac{L_m}{L_s}\left(V_{sd} - \frac{R_s}{L_s}\psi_{sd} + j\omega_r\psi_{sd}\right) \quad (52)$$

$$E_q = \frac{L_m}{L_s}\left(V_{sq} - \frac{R_s}{L_s}\psi_{sq} + j\omega_r\psi_{sq}\right) \quad (53)$$

E_d and E_q represent effect of stator dynamic in rotor current dynamics. It is possible to decouple the cross coupling between the d and q axis components of the rotor current $-j\omega_2\sigma L_r I_{rd}$ and $j\omega_2\sigma L_r I_{rq}$ with the use of rotor current controller [32]. Moreover, a feed forward compensating term is included in the control law that will compensate the tracking error caused by back EMF. Thus the rotor voltage can be stated as:

$$V_{rd} = K_{pid}.e_{rd} + K_{iid}.\int e_{rd}dt + j\omega_2\sigma L_r I_{rd} + K_E.E_d \quad (54)$$

$$V_{rq} = K_{pid}.e_{rq} + K_{iid}.\int e_{rq}dt + j\omega_2\sigma L_r I_{rq} + K_E.E_q \quad (55)$$

where $e_{rd} = I_{rdref} - I_{rd}$ and $e_{rq} = I_{rqref} - I_{rq}$ and K_p and K_i are proportional gain and integral gain. A generic control law KE is introduced to include feed forward compensation term.

$$K_E = \begin{cases} 0 & \text{Without feed forward term} \\ 1 & \text{With feed forward term} \end{cases}$$

Depending on the value of KE compensation level is measured. Introducing active resistance to improve open loop bandwidth of the system, the state equation of rotor current can be stated as:

$$\frac{\sigma.L_r}{\omega_b}\frac{dI_{rd}}{dt} = -R'_r I_{rd} + K_{pid}.e_{rd} + K_{iid}.\int e_{rd}dt + (K_E - 1).E_d - R_a I_{rd} \quad (56)$$

$$\frac{\sigma.L_r}{\omega_b}\frac{dI_{rq}}{dt} = -R'_r I_{rq} + K_{pid}.e_{rq} + K_{iid}.\int e_{rq}dt + (K_E - 1).E_q - R_a I_{rq} \quad (57)$$

The third and fourth term in equation (30) and (31) can be written as:

$$\frac{dX_5}{dt} = K_{iid}..e_{rd} = K_{iid}.(I_{rdref} - I_{rd}) \quad (58)$$

$$\frac{dX_6}{dt} = K_{iid}.e_{rq} = K_{iid}.(I_{rqref} - I_{rq}) \quad (59)$$

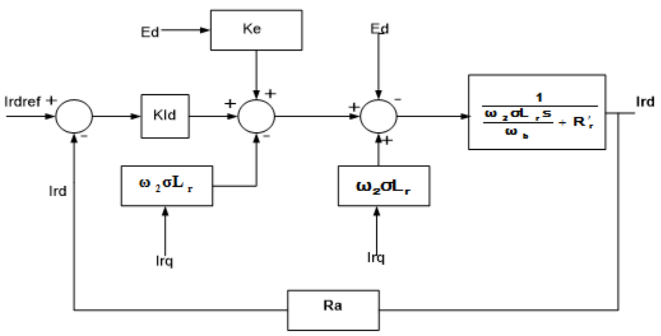

Fig. 7. d-axis rotor current controller with active damping

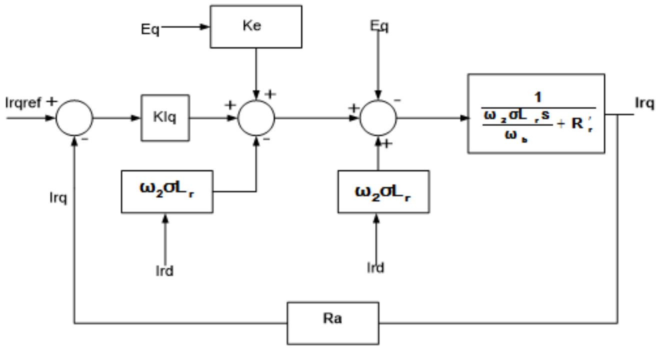

Fig. 8. q-axis rotor current controller with active damping

3.4. Reactive Power Controller

In stator flux orientation, the reactive power and terminal voltage will be controlled by d axis component of rotor voltage and current [33].

$$\alpha_{pf} = \frac{L_m}{L_s}.K_{p\_pf}..\alpha_d.V_s \tag{60}$$

$$K_{i\_pf} = .K_{p\_pf}..\alpha_d. \tag{61}$$

where is the α_{pf} bandwidth of reactive power control loop and is α_d the closed loop bandwidth of d axis rotor current.

Now, the equation for d axis reference current for reactive power controller is stated as:

$$I_{rdref} = -K_{pq}.(Q_{ref} - Q) - \int K_{iq}.(Q_{rref} - Q) \tag{62}$$

$$\frac{dX_8}{dt} = K_{iq}.(Q_{ref} - Q) \tag{63}$$

where Q_{ref} is the reference reactive power, K_{pq} is proportional reactive power gain, and K_{iq} is the integral reactive power gain.

3.5. Speed Controller

In stator flux orientation, the speed will be controlled by q axis component of rotor voltage and current [34].

$$\frac{K_{i\omega}}{K_{p\omega}} = \frac{D}{2H_r}. \tag{64}$$

$$\alpha_\omega = .\frac{L_m}{L_s}..\psi_{so}.\frac{K_{p\omega}}{2H_r} \tag{65}$$

where α_ω is the bandwidth of speed control loop and is α_q the closed loop bandwidth of q axis rotor current.

The equation for q axis reference current is stated as:

$$I_{rqref} = -K_{p\omega}.(\omega_{rref} - \omega_r) - \int K_{i\omega}.(\omega_{rref} - \omega_r) + D_a\omega_r \tag{66}$$

$$\frac{dX_7}{dt} = K_{i\omega}.(\omega_{rref} - \omega_r) \tag{67}$$

4. Dynamic Analysis of Wind and marine Farm

The For fixed tidal speed operation, Squirrel Cage induction generator (SCIG) is considered and dynamic behaviour of this system is simulated using MATLAB/SIMULINK.The parameters chosen for SCIG system are rotor speed, stator voltage, turbine speed and electrical torque.

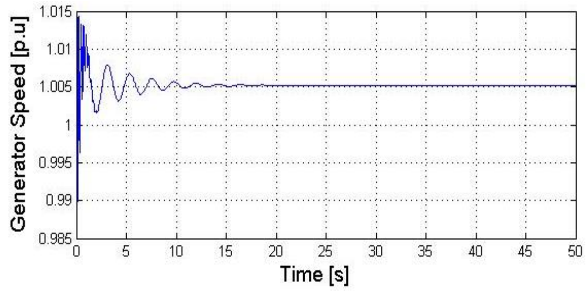

Fig. 9. Generator Speed response

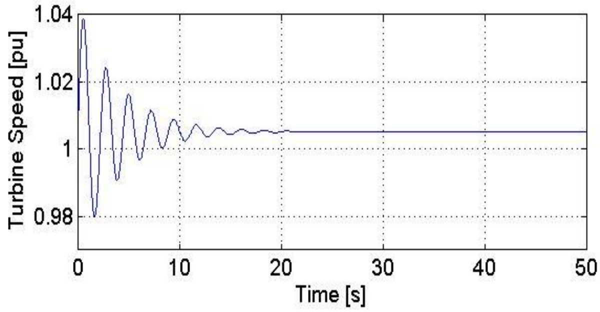

Fig. 10. Turbine speed response

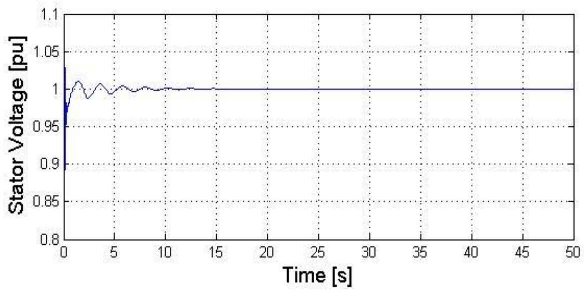

Fig. 18. Stator Voltage response

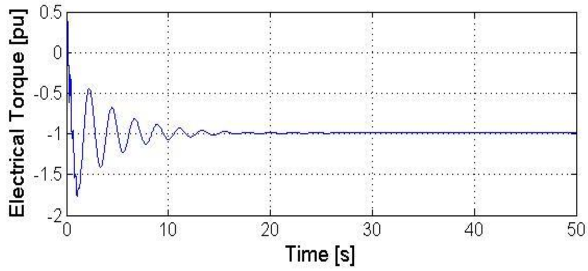

Fig. 11. Electrical Torque response

For variable wind speed operation, Doubly Fed induction generator (DFIG) is considered and dynamic behaviour of this system is simulated using MATLAB/SIMULINK.The parameters chosen for DFIG system are rotor speed, turbine speed, electrical torque and d-axis flux.

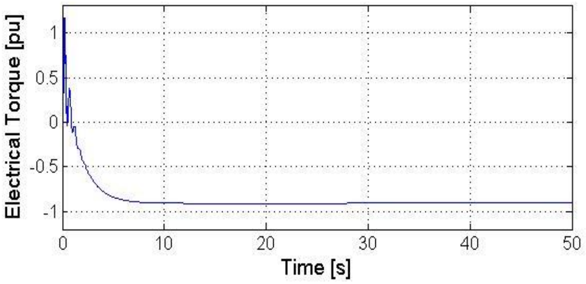

Fig. 12. Electrical Torque response

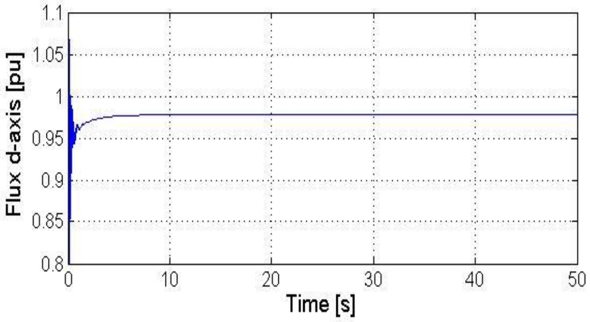

Fig. 13. d-axis flux response

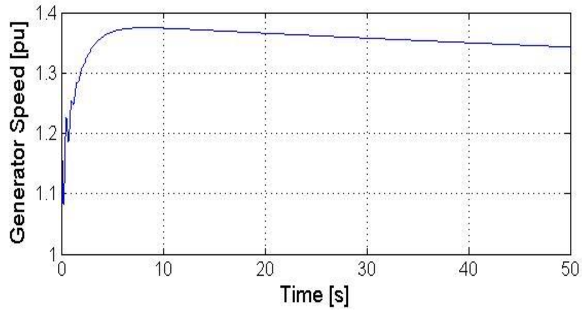

Fig. 14. Generator Speed response

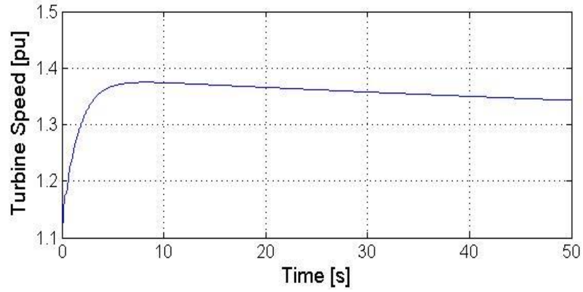

Fig. 15. Turbine Speed response

5. Integrated Topology

The This section presents the proposed small scale model of integrated OWF and MCF which is connected with the existing grid in the mainland or isolated island using high voltage cable. Total capacities of OWF and MCF are considered as 6 and 4 MVA, respectively. OWF is composed of 4 DFIGs of 1.5 MVA each. On the other hand, 4 IGs of MCF are rated at 1 MVA each.

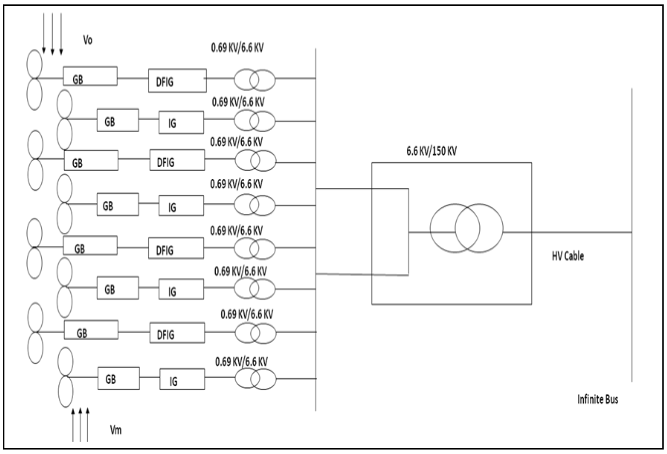

Fig. 16. Integrated topology combining marine current generator and wind turbine generator system

In this scheme, offshore wind and marine current generation units are connected with each other using undersea cable. From the point of connection (PCC) power is transmitted to the grid through offshore step up transformer and high voltage transmission line. The distance between adjacent DFIG and IG of the integrated wind and marine current farm is kept 150 m and distance from PCC and the grid is chosen as 15 km.

5.1. Modal Analysis

In The modal analysis is performed on the hybrid system consisting marine current generator and wind turbine generator. The studied system is linearized around a nominal operating point. Eigenvalues of the studied system are listed in Table 1.

Table 1. Eigenvalue of the integrated system

No.	Eigenvalue	Modes
λ_1	-14.0 + j3906.4	IG electrical mode
λ_2	-14.0 + j3906.4	IG electrical mode
λ_3	-13.1+ j3151.1	IG electrical mode
λ_4	-13.1+ j3151.1	IG electrical mode
λ_5	-376.7	DFIG rotor current mode
λ_6	-373.4	DFIG rotor current mode
λ_7	-5.3+ j373.6	DFIG stator mode
λ_8	-5.3- j373.6	DFIG stator mode
λ_9	-15.5+j376.9	IG stator mode
λ_{10}	-15.5-j376.9	IG stator mode
λ_{11}	-1.8+j24.2	IG electromechanical mode
λ_{12}	-1.8-j24.2	IG electromechanical mode
λ_{13}	-1.6+j13.2	DFIG electromechanical mode
λ_{14}	-1.6-j13.2	DFIG electromechanical mode
λ_{15}	-13.5	DFIG rotor electrical mode
λ_{16}	-13.4	DFIG rotor electrical mode
λ_{17}	-3.8	DFIG real mode
λ_{18}	-4.5	IG monotonic mode
λ_{19}	-0.5-j4.1	IG mechanical mode
λ_{20}	-0.5-j4.1	IG mechanical mode
λ_{21}	-0.5	DFIG weak mechanical mode
λ_{22}	-0.01	DFIG weak mechanical mode

6. Conclusion

The In this paper small signal analysis modelof hybrid topology consisting of fixed speed marine current generator system and variable speed wind turbine generator has been reported. A detailed small signal stability analysis model has been developed for the grid connected fixed speed MTGS which includes two-mass drive train, induction generator, capacitor bank, transmission line. Also a detailed small signal stability model of VSWT including two mass drive train, rotor current controller, speed controller, reactive power controller has been designed. Eventually the main feature of this study is to study small signal analysis of this integrated topology. In the proposed hybrid topology both fixed and variable speed generators are considered where the primary focus was to reduce the investment cost. The modal analysis of the integrated farm is investigated as well as different modes are defined for the integrated topology. A salient co-operate control strategy can also be implemented to stabilize a small scale hybrid power system composed of offshore wind farm and marine current farm during grid fault condition.

References

[1] J. World Energy outlook, International Energy Agencies, pp 303-338, 2010.

[2] “World Wide Energy Report,” Conf. World Wind Energy Renew, Energy Exhib, WWEA, Cairo, pp 6-8, 2010.

[3] “Global Wind Report: Annual Market Update,” Global Wind Energy Council, pp18-19, 2012.

[4] S.E.B. Elghali, R. Balme, K.L. Saux, M.E.H Benbouzid, J.F.Charpentier, and F. Hauville, “A simulation model for the evaluation of the electrical power potential harnessed by a marine current turbine,” IEEE Journal of Oceanic Engineering, vol. 32, no. 4, pp. 786-797, October 2007.

[5] Ozan keysan, Alasdair S. macdonal and Markus Mueller and, “A direct drive permanent magnet generator for a tidal current turbine (SeaGen),” Electric machines and Drive Conference (IEMDC), pp 224-229, 2011.

[6] S. Dahal, N Mithulananthan,, T. Saha, “Investigation of small signal stability of a renewable energy based electricity distribution system,”,Power and Energy Society General Meeting,2010.

[7] PC. Krause, Analysis of Electric Machinery. New York: MacGraw-Hill, 1987.

[8] M. Klein, G.J Rogers,P. Kundur, “A fundamental study of inter-area oscillation in power system,” IEEE Trans. Power System, 6,(3), pp 914-921, 1991.

[9] S Ravichandran, S.G.B Dasan, and R.P.K. Devi, “Small signal stability analysis of grid connected wind energy conversion systems,” International conference on Electrical, Electronics and Control Engineering (ICONRAEeCE), pp 44-50, 15-17 December, 2011.

[10] A Tabesh and R Iravani, “Small-signal dynamic model and analysis of a fixed-speed wind farm-a frequency response,”IEEE Trans. Power Delivery, 21,(2), pp 778-787,2006.

[11] Mohammad Hasanuzzaman Shawon, Ahmed Al-Durra and S.M. Muyeen, “Small signal stability analysis of fixed speed wind generator including SDBR,” XXth International Conference on Electrical Machines (ICEM),2012, pp 2165-2171, 2-5 September, 2012.

[12] Li Xianqi, Zeng Zhiyuan, Zhou Jianzhong, Zhang Yongchuhan, “Small signal stability analysis of large scale variable speed wind turbines integration,” International conference on Electrical machines and systems(ICEMS) , pp 2526-25300, 17-20 October, 2008.

[13] L. Holdsworth X.G. Wu, J.B. Ekanayeke and N. Jenkins,“Comparison of fixed speed and doubly fed induction wind turbine during system disturbances” IEEE Proceeding, Generation, Transmission and distributions., Vol. 15, No. 3, pp.343-352, 2003.

[14] Mohammad Hasanuzzaman Shawon, Ahmed Al-Durra and S.M. Muyeen, “Small signal stability analysis of doubly fed induction generator including SDBR,” 15th International Conference on Electrical Machines and Systems (ICEMS),, pp 1-6, 21-24 October, 2012.

[15] Mohsen Rahimi, Mostafa Parniani, “Dynamic behavior analysis of doubly fed induction generator wind turbines-the influence of rotor and speed controller parameters,” Electrical Power and Energy Systems 32 (2010), pp 464-477.

[16] Y Mishra, S Mishra and F.X Li,“Small signal stability analysis of a DFIG based wind power system under different modes of”, IEEE Trans. Energy conversion. , 24, (4), pp.972-982,2009.

[17] Mohammad Hasanuzzaman Shawon, Ahmed Al-Durra and S.M. Muyeen, “Stability augmentation of interconnected offshore wind and marine current farms,” 37th Annual Conference on IEEE Industrial Electronics Society (IECON 2011), pp 961-966, 7-10 November, 2011.

[18] L. Myers and A. S. Bahaj, “Simulated electrical power potential harnessed by marine current turbine arrays in the Alderney Race,” Renewable Energy,vol. 30, no. 11, pp. 1713-1731, September 2005.

[19] Rahman, M.L., Oka, S., Shirai, Y., "Hybrid Power Generation System Using Offshore-Wind Turbine and Tidal Turbine for Power Fluctuation Compensation (HOT-PC)", Sustainable Energy, IEEE Transactions on, On page(s): 92 - 98 Volume: 1, Issue: 2, July 2010

[20] J. King and T. Tryfonas, “Tidal stream power technology - state of the art,” Oceans 2009-Europe, no. 2, pp. 1-8, May 2009.

[21] Olorunfemi Ojo, “Dynamic and System Bifurcation in Autonomous Induction Generators,” IEEE Transactions Industry Appliactions, Vol 31, pp. 918-924, July/August 1995.

[22] R.C. Bansal, “Three-Phase Self-Excited Induction Generators: An Overview”, IEEE Trans. Energy Conversion, Vol. 2, pp. 292-299, June 2005.

[23] O. Wasynczuk, D. T. Man, J. P. Sullivan,“Dynamic behavior of a class of wind turbine generator during random wind fluctuations,”IEEE Trans. on Power Apparatus and Systems, Vol. PAS-100, No.6, pp.2873-2845, 1981.

[24] K.E. Okedu, S. M. Muyeen,R. Takahashi and J. Tamura, “Stabilization of wind farm by DFIG-based variable speed generators,” International Machines and Systems (ICEMS),2010,pp 464-469.

[25] S. M. Muyeen, Mohd. Hasan Ali, R. Takahashi, T. Murata, J.Tamura, Y. Tomaki, A. Sakahara, and E. Sasano, “A Comparative Study on Transient Stability Analysis of Wind Turbine Generator System Using Different Drive Train Models,” IET-Proceedings on Renewable Power Generation (IET-RPG), Vol.1, No.2, pp.131-141, June, 2007.

[26] Luiz A. C. Lopes, Josselin Lhuilier*, Avishek Mukherjee and Mohammad F. Khokhar, ‘A Wind Turbine Emulator that Represents the Dynamics of the Wind Turbine Rotor and Drive Train ,’ Power Electronics Specialists Conference, 2005. PESC ’05. IEEE 36th. 2005 Page(s): 2092-2097.

[27] T. Senjyu, R. Sakamoto, N. Urasaki, T. Funabashi, H. Fujita and H. Sekine, "Output Power Leveling of Wind Turbine Generator for All Operating Regions by Pitch Angle Control," IEEE Trans. on Energy Conversion., vol. 21, no. 2, pp. 467-475, 2006.

[28] A. Petersson and L. Hamefors and T. Thiringer, "Comparison Between Stator-Flux and Grid-Flux-Oriented Rotor Current Control of Doubly-Fed Induction Generators", Annual IEEE Power Elec. Spec. Conference, 2004.

[29] A. Tapia, G. Tapia, J. X. Ostolaza, and J. R. Saenz, “Modeling and control of a wind turbine driven doubly fed induction generator,” IEEE Trans. Energy Convers., vol. 18, no. 2, pp. 194-204, Jun. 2003.

[30] H. Henao, C. Martis, G.A. Capolino, “An equivalent internal circuit of the induction machine for advanced spectral analysis,” IEEE Trans. Industry Applications, vol. 40, no3, pp.726-734, May/June 2004.

[31] S. Shao, E. Abdi, F. Barati, and R. McMahon, “Stator-flux-oriented vector control for brushless doubly fed induction generator,” IEEE Trans. Ind.Electron., vol. 56, no. 10, pp. 4220-4228, Oct. 2009.

[32] Hu Jia-bing, He Yi-kang, Zhu Jian Guo, "The Internal Model Current Control for Wind Turbine Driven Doubly-Fed Induction Generator", Industry Applications Conference, 2006. 41st IAS Annual Meeting. Conference Record of the 2006 IEEE, On page(s): 209 - 215 Volume: 1, 8-12 Oct. 2006.

[33] Shuhui Li, Haskew, T.A., Williams, K.A., Swatloski, R.P., "Control of DFIG Wind Turbine With Direct-Current Vector Control Configuration", Sustainable Energy, IEEE Transactions on, On page(s): 1 - 11 Volume: 3, Issue: 1, Jan. 2012 .

[34] L. Xu and P. Cartwright. "Direct Active and Reactive Power Control of DFIG for Wind Energy Generation". IEEE Trans. on Energy Conversion ,Vol. 21. NO. 3. Sept. 2006. pp. 750-758.